sciendo

J Vet Res 68, 633-642, 2024
DOI:10.2478/jvetres-2024-0056

The effect of prenatal fumonisin B exposure on bone innervation in newborn Wistar rats

Ewa Tomaszewska[1]✉, Piotr Dobrowolski[2], Aleksandra Dajnowska[3], Liwia Arbatowska[3], Iwona Puzio[1], Halyna Rudyk[4], Oksana Brezvyn[4], Ihor Kotsyumbas[4], Janine Donaldson[5], Jadwiga Śliwa[3], Marcin B. Arciszewski[3], Siemowit Muszyński[6]

[1]Department of Animal Physiology, [3]Department of Animal Anatomy and Histology, Faculty of Veterinary Medicine, [6]Department of Biophysics, Faculty of Environmental Biology, University of Life Sciences in Lublin, 20-950 Lublin, Poland
[2]Department of Functional Anatomy and Cytobiology, Faculty of Biology and Biotechnology, Maria Curie-Sklodowska University, 20-033 Lublin, Poland
[4]State Scientific Research Control Institute of Veterinary Medicinal Products and Feed Additives, 79000 Lviv, Ukraine
[5]School of Physiology, Faculty of Health Sciences, University of the Witwatersrand, Parktown, Johannesburg 2193, South Africa
ewaRST@interia.pl

Received: April 24, 2024 *Accepted: September 23, 2024*

Abstract

Introduction: This study explored the effects of prenatal exposure to fumonisins B (FB) on bone innervation in newborn Wistar rats. **Material and Methods:** Pregnant dams (n = 6 per group) were assigned to either the control or one of two FB-exposed groups (60 mg or 90 mg/kg body weight) from the 7th day of gestation until parturition. On the day of parturition, one male pup from each litter (n = 6 per group) was randomly selected and euthanised, and their femurs were dissected for analysis. Bone innervation was quantified by examining the morphology patterns of sympathetic, parasympathetic, sensory and cocaine- and amphetamine-regulated transcript (CART)-positive fibres. Prepared bone sections were analysed using immunohistochemistry staining for protein gene product 9.5, tyrosine hydroxylase, choline acetyltransferase, vasoactive intestinal peptide (VIP), substance P and CART-positive neurons. **Results:** The group that received a higher dose of FB demonstrated an increase in both the size and complexity of the complete bone neuronal network together with heightened sympathetic and sensory innervation, and displayed a decrease in neuron density and sympathetic innervation. Fumonisin B exposure led to a decrease in galanin-positive and VIP-positive bone neuronal networks in both groups exposed to FB, while in the lower-dose group, there was also a decrease in CART-positive innervation. **Conclusion:** Prenatal FB exposure significantly influences the neuronal bone network of rats, which is essential for maintaining bone homeostasis. These findings emphasise the necessity for further research to understand the lasting effects and underlying mechanisms of alterations induced by FB.

Keywords: mycotoxins, prenatal exposure, bone innervation, peripheral nervous system.

Introduction

Cereals, integral to both human and animal diets, are susceptible to fungal contamination, leading to mycotoxin production that persists in food despite processing (6, 7). Fumonisins (FUM), notably type B (FB1 and FB2), are naturally occurring, prevalent and highly toxic, with FB1 exhibiting slightly greater toxicity than FB2 (depending on the dose of the exposure) and being found naturally in a proportion of about 3:1 to FB2 (23). These mycotoxins are natural byproducts primarily of the metabolism of *Fusarium* but also of *Aspergillus niger* (8). Both types of FB are inhibitors of sphingosine N-acyltransferase, but FB2, a cytotoxic analogue of the more abundant FB1, also inhibits protein serine/threonine phosphatases (6, 7). Fumonisin type B 1 specifically blocks *de novo* sphingolipid biosynthesis through ceramide synthase inhibition.

Different regulations govern the permissible presence of FB1 and FB2 in food and animal feed (8). The clinical consequences of FB exposure in animals are influenced by the route of FB administration and sex and age of the animals, and differ among animal species, with heightened sensitivity being noted in horses, pigs and rodents (7, 13, 27). Non-species-specific symptoms include renal or hepatic toxicity and even hepatocarcinogenic

effects. Species-specific symptoms manifest in target organs, such as the brain in horses, the lungs or oesophagus in pigs (4), and the kidneys in rats, rabbits and sheep (7). The bioavailability and toxicity of FUM are relatively low in ruminants and poultry compared to other species (4, 7). In broiler chickens, clinical toxicity can arise from doses of up to 300 mg/kg feed (7). Fumonisins B disrupt the integrity of the intestinal barrier in poultry at a dose of 1.0 mg/kg body weight (7, 34). Humans exposed to FB risk immunosuppression or neurotoxicity (5, 9, 32). Fumonisin intoxication in humans also results in oesophageal cancers and hepatocarcinoma (14), idiopathic congestive cardiopathy (2, 33) and neural tube defects (NTDs) (18). High incidences of NTDs occur in some regions of the world where substantial consumption of fumonisins has been documented or plausibly suggested (Guatemala, South Africa and China); furthermore, a recent study of NTDs in the border counties of Texas found a significant association between them and consumption of tortillas during the first trimester (19).

The impact on animals due to maternal exposure to FB encompasses disrupted bone homeostasis, altered organ weights and developmental disparities in offspring (38). Maternal FB exposure in rodents results in disturbances in bone metabolic processes, imbalances in the receptor activation of nuclear factor kappa-β ligand (RANKL)/RANK/osteoprotegerin (OPG) and the osteocalcin (OC)/leptin systems (35, 36, 37), or a dose-dependent disturbed erythropoiesis (38). Furthermore, it causes degenerative morphological and structural alterations in the liver and inflammation in striated muscles like the heart and biceps brachii, hormonal imbalances linked with disruptions in the levels of intestinal ghrelin, leptin and their receptors, as well as alterations in the morphology and chemical coding of the enteric nervous system (15, 38). Fumonisins cross the blood-brain barrier and the placental barrier just as other mycotoxins do (5). However, it is believed that their adverse embryonic and foetal effects arise more secondarily from their maternal toxicity (10). They are responsible for genotoxicity, embryotoxicity and neurotoxicity as a result of the disturbance of sphingolipid synthesis and diverse cell-signalling pathways (10, 41), and the neurotoxicity which is peripheral can affect bone innervation. Skeletal development involves coordinated neural infiltration during gestation, with both sensory and autonomic nerve fibres contributing to the established pattern (12). Considering the fundamental mechanism of FUM action, it is noteworthy that sphingolipids form the phospholipid bilayer membrane of neurons and that the lipid composition in the central and peripheral nervous systems is remarkably similar, except for higher levels of sphingomyelin in the peripheral myelin sheath (32).

Understanding the consequences of FUM exposure during pregnancy is crucial for addressing the health challenges in newborn animals and weaned offspring. Taking into consideration the FUM-induced disturbances in the development and function of the enteric nervous system, it would be logical to direct research towards understanding the effects of FUM on peripheral innervation – exploring if and how FUM might disrupt the bone nervous system network. Given the already established negative effects of FUM on bone homeostasis (bone weakening and loss), research should extend beyond basal bone histomorphometry and turnover of protein in the matrix and should focus on investigating potential disruptions in the bone nervous system caused by FUM.

In line with the hypothesis of the prenatal origin of health and disease (foetal programming) (22), it has been proposed that prenatal exposure to FUM not only influences bone metabolism and microstructure but also has the potential to alter the chemical coding of bone nerves, leading to compromised bone homeostasis and development. Therefore, this study aimed to assess how maternal oral FB exposure affects bone innervation in newborn rat offspring. In particular, this investigation focused on alterations in sympathetic, parasympathetic and sensory bone innervation. These analyses are of paramount importance to deepen our understanding of the effects of FB exposure during pregnancy on compromised postnatal bone development.

Material and Methods

Fumonisins. The FB utilised in this study were generated *in vitro* on maize kernels using *F. verticillioides* sourced from the biobank at the Institute of Veterinary Medicine of the National Academy of Agrarian Sciences, Kiev, Ukraine as described previously (34). Briefly, the cultures were grown on the maize substrates for a duration of four weeks. Contaminated grains underwent analysis for FB1 and FB2 content using liquid chromatography in accordance with the AOAC method #2001.04 (1); the National Veterinary Research Institute in Puławy, Poland, analysed the maize. The analysis confirmed a 3:1 ratio of FB1 to FB2 (73% and 27%, respectively). The FB were extracted from the ground maize using ethanol, quantified *via* a commercial ELISA kit (RIDASCREEN Fumonisin; R-Biopharm, Darmstadt, Germany), and the extract was then concentrated to a stock solution of 100 mg of FB1+FB2 per mL. Throughout the experiment, the stock solution was diluted with 0.5 mL of 0.9% saline to achieve the desired concentrations for administration based on the daily weight measurements of each pregnant dam. The median lethal dose (LD_{50}) value was established based on developmental studies previously conducted at the State Scientific Research Control Institute of Veterinary Medicinal Products and Feed Additives in Lviv, Ukraine (26).

Animals and experimental design. The study involved eighteen pregnant, six-week-old Wistar rat dams. The dams were individually housed in polypropylene cages at a temperature of 21 ± 3°C, in

relative humidity of 55 ± 5% and a 12h/12h light/dark cycle. The rats were randomly assigned to one of three groups (n = 6 each): to a control group (group I) not treated with FB, or to one of two groups intoxicated with FB, either at a dose of 60 mg FB/kg body weight (b.w.) (group II) or 90 mg FB/kg b.w. (group III). A dose of 60 mg FB/kg b.w., an equivalent to 1/15 of the established LD_{50}, has been shown not to lead to clinical or subclinical symptoms in adolescent rats, while a dose of 90 mg FB/kg b.w., constituting 1/10 of the LD_{50}, has been shown to induce subclinical intoxication in adolescent rats (26). Fumonisins B were administered *via* intragastric gavage in a volume of 0.5 mL of 0.9% saline solution, starting from the 7th day of gestation until parturition, as previously described (35, 36, 37). Control animals were given an equivalent volume of saline solution using the same method. Dams were allowed free access to drinking water and fed standard laboratory rodent chow (Ssniff Spezialdiäten, Soest, Germany) which met the American Institute of Nutrition AIN-93 nutritional requirements. On the day of parturition, to exclude litter effects on the results, only one male pup from each litter was randomly selected to be euthanised *via* CO_2 inhalation for subsequent analyses. The sex of the selected pups was confirmed by inspecting primary sexual characteristics after opening the abdominal cavity. The right femora were dissected and the bones were then fixed in phosphate-buffered paraformaldehyde (4% v/v, pH 7.0). The selection of the male sex for analysis in this study was informed by previous research on bone innervation (31). To assess FB mother toxicity, after dams` euthanasia, the weight of dams and their livers, the aspartate aminotransferase (AST) and alanine aminotransferase activity, and the sex ratio in the litters were determined.

Immunohistochemistry. After fixation, paraffin-embedded, 4-µm-thick sections were rehydrated and treated with proteinase K for 30 min at room temperature (RT) to retrieve antigens. A 3% H_2O_2 solution was applied for 5 min to inhibit the endogenous peroxidase activity. To reduce nonspecific binding, sections were blocked for 30 min using UltraCruz Blocking Reagent (sc-516214; Santa Cruz Biotechnology, Dallas, TX, USA). For visualising the bone nervous system, a wide range of primary antibodies was used. For the general bone innervation pattern, it was protein gene product 9.5 (PGP9.5) monoclonal rabbit antibody (ab108986; Abcam, Cambridge, UK, at 1:1,000 dilution); for sympathetic bone innervation it was tyrosine hydroxylase (TH) monoclonal mouse antibody (22941; ImmunoStar, Hudson, WI, USA, at 1:1,000 dilution); for parasympathetic bone innervation the reagents were choline acetyltransferase (ChAT) monoclonal rabbit antibody (ab178850; Abcam, at 1:1,000 dilution) and vasoactive intestinal peptide (VIP) polyclonal rabbit antibody (ab22736; Abcam, at 1:1,200 dilution); the antibodies for sensory bone innervation were substance P (SP) monoclonal mouse (ab14184; Abcam, at 1:1,000 dilution) and galanin (GAL) monoclonal rabbit immunoglobulins (ab254556; Abcam, at 1:4,000 dilution); and the CART-positive bone innervation antibody was a cocaine- and amphetamine-regulated transcript (CART) polyclonal rabbit product (H-003-61; Phoenix Pharmaceuticals, Burlingame, CA, USA, at 1:10,000 dilution). Immunohistochemical staining was performed overnight at 4°C. After primary antibody incubation, the sections were treated at RT with a polyclonal horseradish peroxidase goat anti-mouse/rabbit immunoglobulin G detection system (DPVB110HRP; Immunologic WellMed, Duiven, the Netherlands). Visualisation was achieved with a 3,3′-diaminobenzidine (DAB) chromogen (D5905; Sigma-Aldrich, St. Louis, MO, USA) followed by haematoxylin counterstaining (MHS32; Sigma-Aldrich).

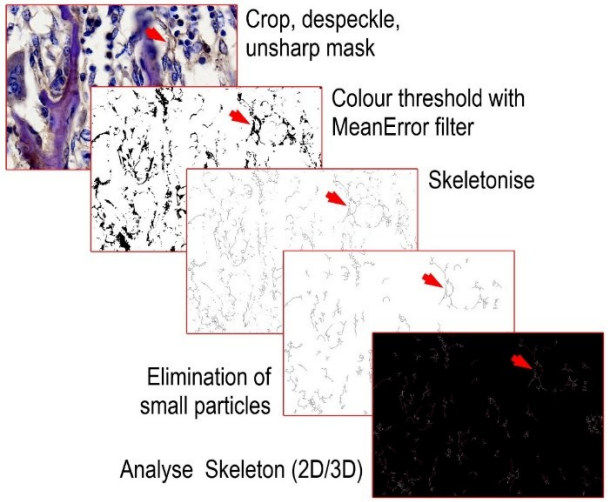

Fig. 1. A diagram showing the graphical analysis steps for image segmentation and bone neuronal net analysis. Red arrows indicate an example of an identified neuronal element in subsequent processes of image transformation

Image analysis. Evaluation of changes in neuronal morphology and their spatial distribution was carried out with image material and was based on the methodology described by Marques *et al.* (20). Images were acquired using a CX43 light microscope (Olympus Life Science, Tokyo, Japan) equipped with a 20× S Plan Apo objective and SC50 4,912 × 3,684 pixel digital microscope camera (Olympus). Images were saved in the TIF format to ensure high-resolution data for subsequent analysis. Image analysis was performed using Fiji-ImageJ 1.54f (28) with its image processing pipeline of calibration for accurate measurements, noise reduction, and linking of dark pixels to improve the image quality. A key aspect of this analysis was the application of carefully designed colour thresholding using the MeanError filter, which allowed selective identification of DAB-stained neurons and effectively eliminated non-neuronal background elements. Following the thresholding step, a skeletonisation process was applied to streamline neuronal structures while preserving their essential morphological features. The Skeletonize (2D/3D) and Summarize Skeleton plugins for Fiji were used to extract relevant information from the images (Fig. 1).

The comprehensive image analysis approach allowed the quantification of critical parameters relevant to studies on neural morphology, connectivity or the studied substances' toxicity to neuronal structures. The first parameter was the spatial distribution of neurons (%): a quantitative assessment of the spatial distribution of all elements of neurons within the studied region and insights into the arrangement, clustering or dispersion of these neurons in the bone. The second was the mean cross-sectional area of neuronal protrusions (µm²): a quantitative assessment of the cross-sectional area occupied by neuronal bodies and their protrusions including dendrites and axons. The cross-sectional density of neuronal protrusions (per mm²) was the next parameter: the number of intersected or cut neuronal protrusion cross-sections within a defined area. The mean length of the neuronal tree (µm) was also calculated: the mean length of the dendritic and axonal arbours, collectively referred to as "neuronal trees" in neurons. The final parameter was the mean number of branches (per neuron): the average count of branches in individual neurons, quantifying the branching complexity of neurons.

Statistical analysis. Analyses were conducted using GraphPad Prism software v. 10.0.2 (GraphPad Software, San Diego, CA, USA). A Shapiro–Wilk test validated that the data were normally distributed, and variance homogeneity was confirmed using the Brown–Forsythe test. A one-way analysis of variance was employed, with post-hoc analysis by Tukey's honest significant difference test. Statistical significance was established at P-value < 0.05.

Results

Maternal toxicity. No changes in the behaviour or basal health state of the pregnant dams were observed during assessments by a veterinarian. Food and water consumption remained consistent across all groups of dams regardless of the treatment they received. In the current study, a decrease in the body weight of dams was only observed after exposure to 90 mg FB/kg b.w. (Fig. 2a). Both FB doses led to a reduction in the liver weight of dams (Fig. 2b and c) and an increase in the activity of AST (Fig. 2d), a non-organ-specific enzyme commonly associated with skeletal and heart muscles as well as with the liver. No FB effect on litter size (Fig. 2f) or sex ratio in the litter (Fig. 2g) was observed, but the terminal body weight of offspring of both sexes was reduced in the FB-administrated groups (Fig. 2h–j).

General bone innervation pattern. Protein gene product 9.5 was used to quantify the complete bone neuronal network, which innervates the periosteum, cortical and trabecular bones, and bone marrow. The network underwent a significant change in its spatial distribution (Fig. 3). Exposure to the lower dose of FB led to a significant extension of the spatial distribution of the neuronal network compared to that in both the control and higher-dose groups.

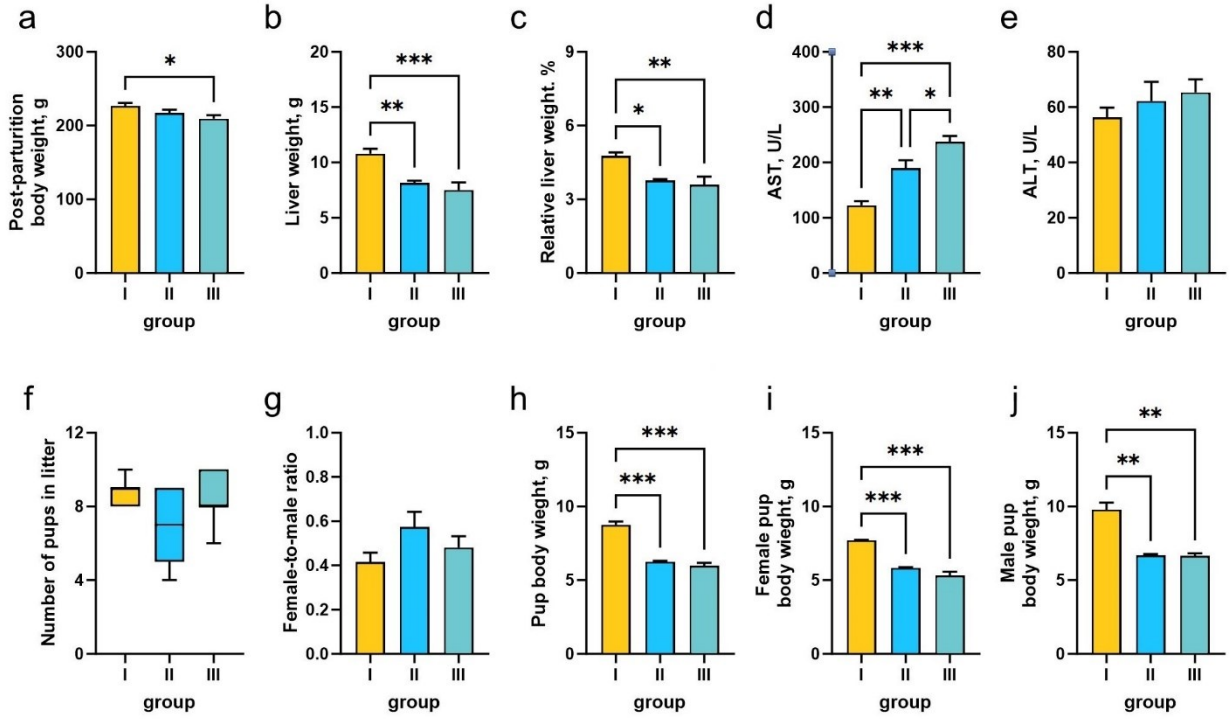

Fig. 2. Effects of fumonisin exposure on Wistar rat dams. a – post-parturition body weight; b – liver weight; c – relative liver weight (percentage of total body weight); d – serum aspartate aminotransferase (AST) activity; e – serum alanine aminotransferase (ALT) activity; f – litter size (number of live pups); (g) – offspring sex ratio (female-to-male); h – average pup body weight; i – female pup body weight; j – male pup body weight. Group I – control group; Group II – dams intoxicated with 60 fumonisins B (FB)/kg b.w. during gestation; Group III – dams intoxicated with 90 FB/kg b.w. during gestation. The data are presented as mean values ± standard error of the mean (n = 6), except for (f), where the line indicates the median, the box represents the interquartile range, and the whiskers show minimum and maximum value ranges. * – statistical significance at P-value < 0.05; ** – P-value < 0.01; *** – P-value < 0.001

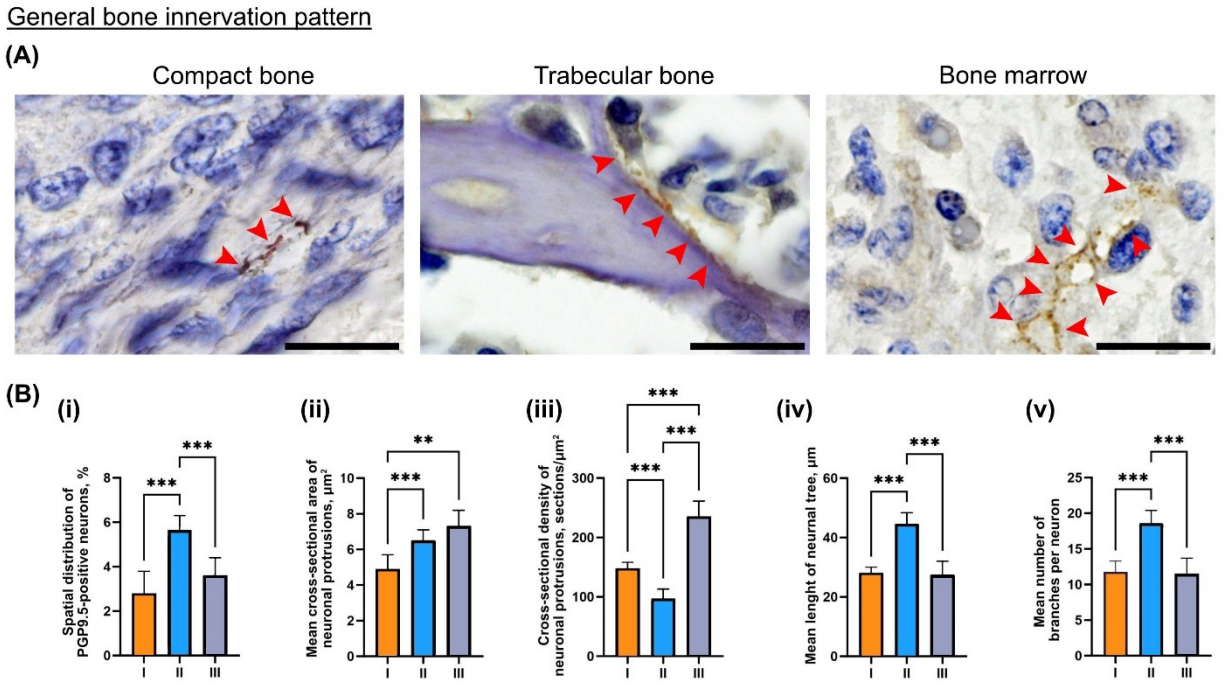

Fig. 3. Effects of prenatal fumonisins exposure on general bone innervation: A – representative photomicrographs showing protein gene product 9.5 (PGP9.5)-positive neuronal nets (arrowheads) in compact bone, trabecular bone and bone marrow; B – general bone innervation pattern quantified by morphology of the PGP9.5-positive neurons: i – spatial distribution of PGP9.5-positive neurons; ii – average cross-sectional area of PGP9.5-positive neuronal protrusions; iii – neuronal protrusion cross-sectional density of PGP9.5-positive neurons; iv – average length of neuronal trees in PGP9.5-positive neurons; v – mean number of branches in PGP9.5-positive neurons. Group I – control group; Group II – newborns from dams intoxicated with 60 fumonisins B (FB)/kg b.w. during gestation; Group III – newborns from dams intoxicated with 90 FB/kg b.w. during gestation. The data are presented as mean values ± standard error of the mean (n = 6); * – statistical significance at P-value < 0.05; ** – P-value < 0.01; *** – P-value < 0.001; scale bars – 20 µm

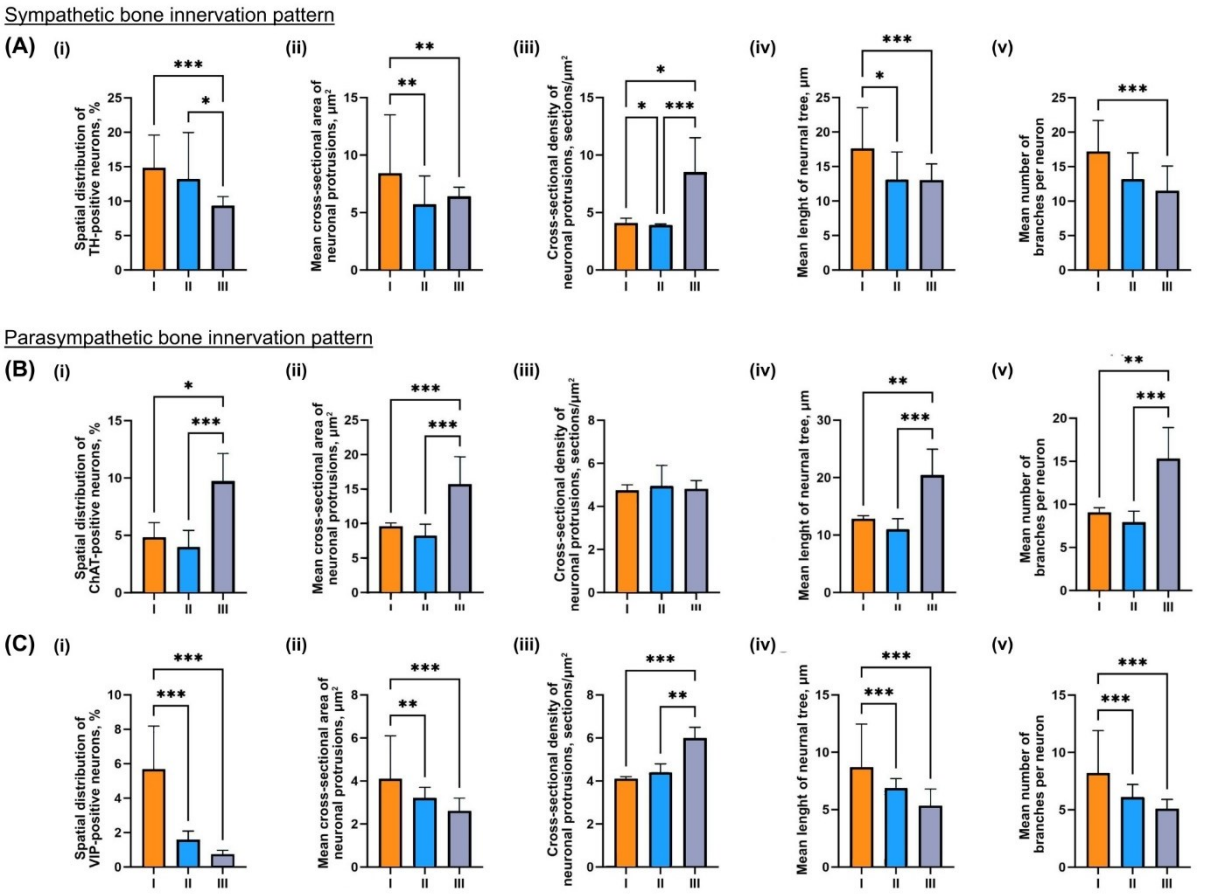

Fig. 4. Effects of prenatal fumonisin exposure on bone innervation: A – sympathetic and B and C – parasympathetic patterns quantified by morphology of the immunoreactive (IR) neurons. A – tyrosine hydroxylase (TH)-positive; B – choline acetyltransferase (ChAT)-positive; C – vasoactive intestinal peptide (VIP)-positive neurons: i – spatial distribution of IR neurons; ii – average cross-sectional area of IR neuronal protrusions; iii – neuronal protrusion cross-sectional density of IR neurons; iv – average length of neuronal trees in IR neurons; v – mean number of branches in IR neurons. Group I – control group; Group II – newborns from dams intoxicated with 60 fumonisins B (FB)/kg b.w. during gestation; Group III – newborns from dams intoxicated with 90 FB/kg b.w. during gestation. The data are presented as mean values ± standard error of the mean (n = 6); * – statistical significance at P-value < 0.05; ** – P-value < 0.01; *** – P-value < 0.001

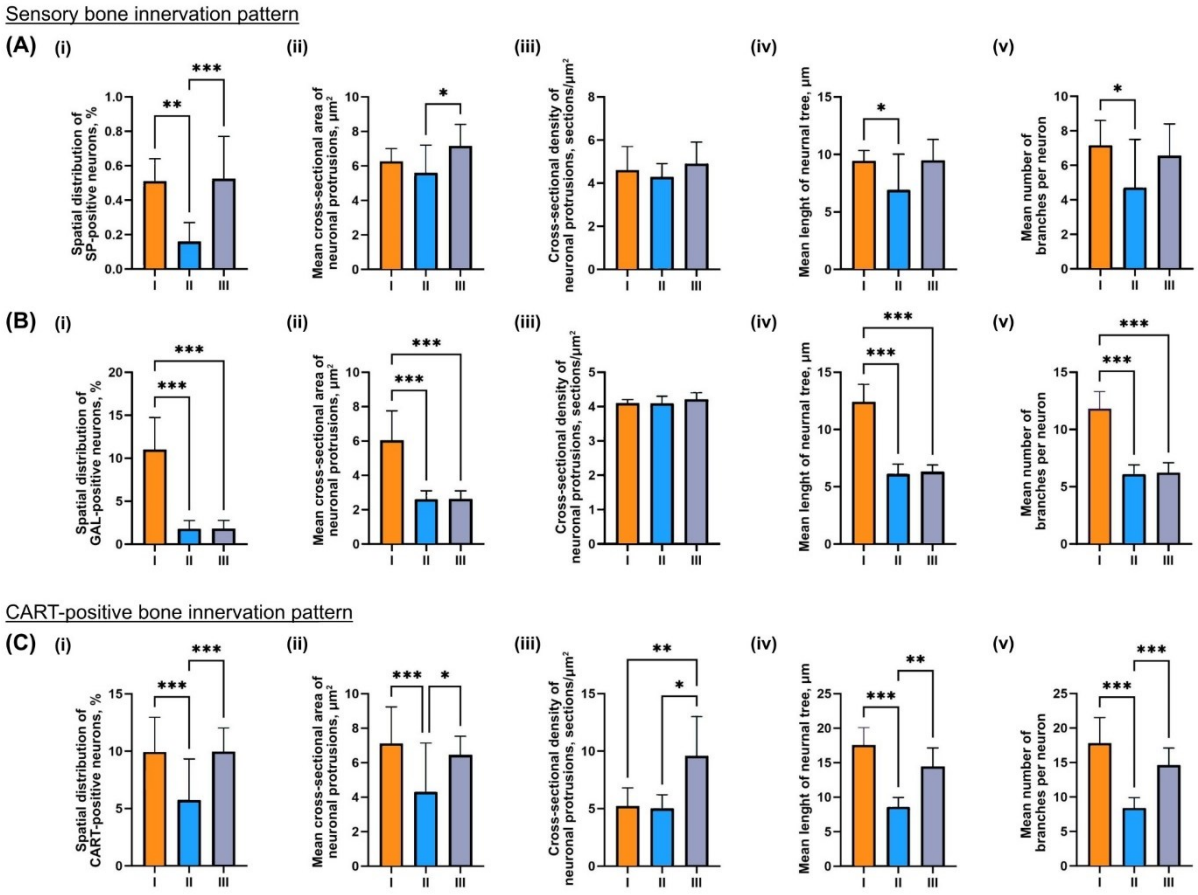

Fig. 5. Effects of prenatal fumonisins exposure on bone innervation: A and B – sensory and C – cocaine- and amphetamine-regulated transcript (CART)-positive patterns quantified by morphology of the immunoreactive (IR) neurons. A – SP-positive; B – GAL-positive; C – CART-positive neurons; i – spatial distribution of IR neurons; ii – average cross-sectional area of IR neuronal protrusions; iii – neuronal protrusion cross-sectional density of IR neurons; iv – average length of neuronal trees in IR neurons; v – mean number of branches in IR neurons. Group I – control group; Group II – newborns from dams intoxicated with 60 fumonisins B (FB)/kg b.w. during gestation; Group III – newborns from dams intoxicated with 90 FB/kg b.w. during gestation. The data are presented as mean values ± standard error of the mean (n = 6); * – statistical significance at P-value < 0.05; ** – P-value < 0.01; *** – P-value < 0.001

The mean cross-sectional area of the protrusions throughout the network expanded after exposure to FB, regardless of dose. However, the cross-sectional density of neuronal processes showed a nuanced response, decreasing after exposure to the lower dose and increasing after exposure to the higher dose. After exposure to the lower dose of FB, neuronal morphology and the mean length of neuronal trees and number of branches per neuron significantly increased compared to both the control and the higher-dose exposure groups.

Sympathetic bone innervation pattern. Analysis of the TH-positive neuronal network (Fig. 4A), as demonstrated by the spatial distribution of TH-positive neurons, showed a significant reduction in TH-positive neurons in the femora of pups exposed to the higher dose of FB compared to the femora of control group pups and those of the group exposed to the lower dose. The smaller mean cross-sectional area of protrusions and shorter mean length of neuronal trees within the TH-positive neuronal network after exposure to either dose of FB indicated a diminished impact area on the bone tissue overall. The cross-sectional thickness of the TH-positive cell protrusions showed intricate regulatory mechanisms. Exposure to the higher dose of FB increased the cross-sectional density, in contrast to the control and lower-dose groups. The density was lower in the lower-dose group than in the control group. Similarly, there were fewer branches on average per TH-positive neuron in the bones of pups exposed to the higher dose of FB, implying a narrow impact zone.

Parasympathetic bone innervation pattern. The parasympathetic bone neuronal network was evaluated using ChAT (Fig. 4B) and VIP (Fig. 4C). The spatial distribution of ChAT-positive neurons in the higher-dose exposure group exceeded that of both the control group and the lower-dose exposure group, and this difference was considered statistically significant. The presence of more ChAT-positive neurons suggests amplified parasympathetic influence on bone regulation. Examination of ChAT-positive neuronal network parameters revealed a greater mean cross-sectional area of protrusions, length of neuronal trees and number of branches per neuron after the higher FB dose. Several parameters related to the VIP-positive neuronal network were lower because of exposure to FB, including the average area of VIP-positive neuronal protrusions, length of neuronal trees in the VIP-positive neuronal network and number of branches per VIP-positive

neuron, which was accompanied by a rise in the cross-sectional density of neuronal protrusions.

Sensory bone innervation pattern. The neuronal network exhibiting SP-positive characteristics (Fig. 5A) was notably smaller in the lower-dosed group than in the control and higher-dosed groups. These findings indicated that the lower dose of FB resulted in a significant size reduction in the SP-positive neuronal network. The observed decrease implied a contraction of the affected area and emphasised the intricate relationship between bone cells and SP-positive neurons. The average cross-sectional area of SP-positive neuronal protrusions in the femora of the pups exposed to the higher dose of FB was larger than that in the femora of the pups exposed to the lower dose. The average length of the neuronal tree in the SP-positive neuronal network and the mean number of branches per SP-positive neuron were diminished following exposure to the lower dose of FB compared to this length and number following only saline solution administration. This, coupled with the absence of changes in cross-sectional density of neuronal protrusions, suggests a reduction in impact area. The components of the sensory bone neuron network were also examined using a GAL marker (Fig. 5B). The distribution of GAL-positive neurons in the spatial domain was sparser in the FB-exposed bones, irrespective of the administered dose. A decrease in GAL-innervation was observed as a simplification of the neuronal structure, which could have significant implications for the intricate relationship between GAL-positive neurons and bone cells. It is worth noting that the mean cross-sectional area of GAL-positive neuronal protrusions, mean length of neuronal trees in the GAL-positive neuronal network, and mean number of branches and end-points per GAL-positive neuron decreased after exposure to FB, with no observable dose dependency. Similarly to the SP-positive network, the GAL-positive neuronal network's protrusion cross-sectional density was unaffected by exposure to FB, despite the simplified structure. These alterations suggest that the structure of GAL-innervation had been simplified, which could potentially impact the development and remodelling of the bone tissue. The present results demonstrated a very strong impact of FB on the GAL-positive network in the bones of newborn rats, irrespective of the dose used.

CART-positive bone innervation pattern. In the present investigation of the neural network exhibiting CART-positivity (Fig. 5C), a notably smaller spatial distribution of CART-expressing neurons was observed in bones exposed to the lower dose of FB, compared to unexposed bones and bones exposed to the higher dose. The results indicated a greater impact on the bone region at the lower dose, as evidenced by a significant reduction in the average cross-sectional area of CART-positive neuronal protrusions, mean length of neuronal trees in the CART-positive neuronal network and mean number of branches in CART-positive neurons after exposure to a lower dose of FB than after exposure to none and to the higher dose. In contrast, the cross-sectional density of neuronal protrusions noted in the femora of the more intoxicated pups significantly exceeded the density in the femora of both the control pups and the less intoxicated pups.

Discussion

An experiment with a scope similar to that presented in this publication has not been conducted previously. Therefore, discussing and comparing results is challenging and at times even impossible. The only available information is regarding the impact of FUM on the central nervous system. One study showed dose- and region-dependent alterations in neurotransmitters (norepinephrine and dopamine) and their metabolites (39). Equine leukoencephalomalacia is a fatal degenerative disease and another example of FUM neurotoxicity affecting the central nervous system. This intoxication results in metabolic disturbances that lead to the softening and liquefaction of the white matter in the brain, which is rich in sphingomyelin (25). Thus, the hypothesised peripheral neurotoxicity of FB to bone appears to be in line, at least to some extent, with existing evidence. Kras *et al.* (15) previously presented the harmful impact of prenatal exposure to FUM on the enteric nervous system. Although somewhat related research is described in the literature, the effects of foetal exposure to FUM on bone innervation have not been examined previously. The peripheral nervous system has a strong impact on the maintenance of bone homeostasis. The distribution and function of specific postganglionic neuronal populations within the bone are well established. In the current study, numerous fibres with immunoreactivity for commonly accepted markers for four types of innervation have been found in the entire bone (TH for sympathetic; ChAT for parasympathetic; SP, GAL and VIP for sensory; and CART). The results of the present study indicate a dose-dependent effect of FB on CART-positive networks and seem to be in agreement with previous findings relating to the RANKL/RANK/OPG system and bone loss in newborn and weaned rats prenatally exposed to FUM (36, 37).

Fumonisins induce a range of adverse effects, the extent and nature of which are contingent upon factors such as dosage, duration of exposure and the specific stage of foetal development during which exposure occurs (3). Their maternal effects are currently under consideration by the European Food Safety Authority (6). The maternal, embryonic and foetal toxicity of FUM poisoning have been studied for decades. Collins *et al.* (3) used 0, 15, 30, 60 and 120 mg/kg b.w. to intoxicate pregnant rats from gestational day 3 to 16. Riley *et al.* (24) used pure FB1 at 0, 5, 10, 15, 25 and 50 mg/kg b.w. per day for three consecutive days on embryonic days (ED) 6.5, 7.5 and 8.5. The current findings on maternal toxicity align with the results of

another study conducted on Fischer 344 rats exposed to 60 mg FB1/kg b.w. between the 8th and 12th days of pregnancy. In that study, FB1 was shown to decrease litter weight, but no significant effect on weight gain in dams was observed (16).

The sympathetic bone innervation pattern shows that sympathetic (TH) neurons make contact with various cell types, including osteoblasts, osteoclasts, hematopoietic cells and endothelial cells of blood vessels within the bone marrow *via* beta-adrenergic receptors. The current study revealed that prenatal exposure to FB significantly decreased the TH-positive neuronal network in newborn rats, regardless of the administered dose. Cholinergic nerves regulate osteoblast proliferation and differentiation, prenatal bone development, postnatal ossification and bone formation (30). Moreover, osteoclast activity is affected by the release of VIP and acetylcholine. Vasoactive intestinal peptide inhibits osteoblast activity (17), acts on haematopoietic progenitors and bone marrow stem cells, and regulates their release of vascular endothelial growth factor (VEGF), which promotes the angiogenesis needed for proper development. Our observations are in line with previous results showing changes in bone VEGF expression in rats prenatally exposed to FUM (35). However, not all cholinergic fibres can release VIP; therefore, the changes observed within the VIP-positive neuronal network cannot be linked with the changes observed in the ChAT-positive neuronal network. In this study, exposure to FB had a significant effect on the VIP-positive neuronal network. Given the established role of VIP innervation in osteoclast activity, lowering of several VIP-innervation parameters could potentially lead to beneficial effects. Taken together, the roles of sympathetic innervation and VIP in bone homeostasis and the observed changes in bone innervation in the current study allowed us to conclude that the present results are consistent with the previously demonstrated effect of prenatal exposure to FUM on the activity of osteoblasts and osteoclasts, which causes modifications in the RANKL/RANK/OPG system and the synthesis of non-collagenous bone proteins in both newborn and weaned rats (36, 37).

Additionally, detriment to bone integrity is caused by the alterations in bone non-collagenous protein composition caused by the function of osteoblasts becoming compromised because of alterations in the ChAT-positive neuronal network after prenatal FB exposure. These alterations translate into compromised mechanical and geometric properties, which have previously been described (26). The restricted availability of literature hinders a more comprehensive discussion of this aspect. Substance P has a significant impact on bone metabolism by promoting RANKL production by osteoblasts (29). The RANKL/RANK/OPG system is adversely affected by prenatal exposure to FUM (36, 37). The current study demonstrated a strong dose-dependent effect of FB on the SP-positive network, which is also involved in bone nociception, pain being felt differently in the case of bone fractures involving the periosteum, mechanical loading or bone tumours (21). The present study also focused on the CART network involving neuropeptides. These neuropeptide receptors have not yet been described; however, some data indicate that CART regulates bone resorption by enhancing RANKL (29). The present analysis included not only the neuronal network of bone tissue (compact and trabecular bone) with the periosteum but also the bone marrow, which is an important haematopoietic and lymphoid organ. The role of sympathetic innervation in myelopoiesis and platelet formation is well established and has an inhibitory effect opposite to that observed in haematopoiesis after parasympathetic stimulation. Substance P-positive nerves are also abundant in the bone marrow and influence blood flow, stem cell release, cytokine production and cell differentiation and proliferation of cells, indicating that this type of innervation plays a significant role in haematopoiesis (40). A previous study revealed changes in basal blood morphology (a fall in white blood cells and a rise in red blood cells) and a possible FB effect on haematopoietic cells in weaned rats prenatally exposed to the same doses of FB (38). Previous and current results have demonstrated the undeniable impact of FB on the processes involved in the production of various blood morphometric components. The findings of Tomaszewska *et al.* (38 suggest that this effect may be long-lasting, as these changes were observed in weaned rats that were no longer exposed to FB. Moreover, all observed changes in bone innervation in the offspring of mothers exposed to FB during pregnancy, regardless of the dose, demonstrated the plasticity of the peripheral nervous system. The observed enlargement of the bone neuronal tree in the current study may be a compensatory reaction to the altered expression of neurotransmitters resulting from damage to nerve fibres caused by FB exposure.

Nevertheless, pinpointing the primary causative factor for the observed alterations in bone innervation remains challenging. Specifically, it is unclear whether these effects stem from maternal toxicity or direct exposure to the embryo. Studies involving rodent models indicate that FUM can traverse the placenta during a specific embryonic period (ED 7.5–8.5) when the placenta is not fully developed (11). Effects during this period are considered direct impacts on the embryo, separate from maternal toxicity. Exposure at various stages may result in alterations in foetal tissue due to maternal toxicity. While the present study addressed this crucial period (albeit for 1.5 days) for direct effects and addressed the time when effects might be deemed indirect and due to maternal toxicity, further investigation is necessary. The study also has some limitations, such as the determination not having been made of FB in the livers of mothers and newborns or of the effects of fumonisins on sphingolipids in the mother and in the newborns.

Conclusion

This study unequivocally demonstrates neurotoxic effects following prenatal exposure to FB. Significant alterations in sympathetic, sensory and CART-positive fibres underscore the critical role of FB in modulating essential neuronal networks crucial for bone homeostasis. Although this study clearly establishes a dose-dependent effect of prenatal FB exposure on bone innervation in newborns, further research is essential to elucidate the underlying mechanisms and long-term implications of these changes, particularly at different doses not explored in this study.

Conflict of Interests Statement: The authors declare that there is no conflict of interests regarding the publication of this article.

Financial Disclosure Statement: This research was co-financed by the Polish National Agency for Academic Exchange (NAWA, Poland), grant no. PPN/BUA/2019/1/00024/U/00001, Polish National Science Centre (NCN, Poland) grant no. 2022/01/3/NZ9/00123, and the Ministry of Education and Science of Ukraine, grant No. 0120U104053 (M/89-2020).

Animal Rights Statement: The experiment was conducted under the license of the Ethical Committee of the State Scientific Research Control Institute of Veterinary Medicinal Products and Feed Additives in Lviv, Ukraine (permission No. 132 676-Adm/08/2020). Although it took place in a non-EU country, special attention was paid to ensure that the study adhered to the guidelines set forth in EU Directive 2010/63/EU concerning the protection of animals used for scientific purposes.

References

1. Association of Official Analytical Chemists: AOAC Method 2001.04-2001, Fumonisins B1 and B2 in corn and corn flakes, 19th edition, AOAC International, Gaithersburg, MD, USA, 2012.
2. Chen J., Wen J., Tang Y., Shi J., Mu G., Yan R., Cai J., Long M.: Research Progress on Fumonisin B1 Contamination and Toxicity: A Review. Molecules 2021, 26, 5238, doi: 10.3390/molecules26175238.
3. Collins T.F.X., Sprando R.L., Black T.N., Shackelford M.E., Laborde J.B., Hansen D.K., Eppley R.M., Trucksess M.W., Howard P.C., Bryant M.A., Ruggles D.I., Olejnik N., Rorie J.I.: Effects of Fumonisin B1 in Pregnant Rats. Part 2. Food Chem Toxicol 1998, 36, 673–685, doi: 10.1016/S0278-6915(98)00036-2.
4. Devreese M., De Backer P., Croubels S.: Overview of the most important mycotoxins for the pig and poultry husbandry. Vlaam Diergeneeskd Tijdschr 2013, 82, 171–180, doi: 10.21825/vdt.v82i4.16694.
5. Domijan A.-M.: Fumonisin B1: A Neurotoxic Mycotoxin. Arh Hig Rada Toksikol 2012, 63, 531–544, doi: 10.2478/10004-1254-63-2012-2239.
6. European Food Safety Authority Panel on Contaminants in the Food Chain (CONTAM), Knutsen H.-K., Alexander J., Barregård L., Bignami M., Brüschweiler B., Ceccatelli S., Cottrill B., DiNovi M., Edler L., Grasl-Kraupp B., Hogstrand C., Hoogenboom L.R., Nebbia C.S., Petersen A.; Rose M., Roudot A.-C., Schwerdtle T., Vleminckx C., Vollmer G., Wallace H., Dall'Asta C., Eriksen G.-S., Taranu I., Altieri A., Roldán-Torres R., Oswald I.P.: Risks for animal health related to the presence of fumonisins, their modified forms and hidden forms in feed. EFSA J 2018, 16, 144, doi: 10.2903/j.efsa.2018.5242.
7. European Food Safety Authority Panel on Contaminants in the Food Chain (CONTAM), Schrenk D., Bignami M., Bodin L., Chipman J.K., del Mazo J., Grasl-Kraupp B., Hogstrand C., Leblanc J.C., Nielsen E., Ntzani E., Petersen A., Sand S., Schwerdtle T., Vleminckx C., Wallace H., Daenicke S., Nebbia C.S., Oswald I.P., Rovesti E., Steinkellner H., Hoogenboom L.R.: Assessment of information as regards the toxicity of fumonisins for pigs, poultry and horses. EFSA J 2022, 20, 7534, doi: 10.2903/j.efsa.2022.7534.
8. Gao Z., Luo K., Zhu Q., Peng J., Liu C., Wang X., Li S., Zhang H.: The natural occurrence, toxicity mechanisms and management strategies of Fumonisin B1: A review. Environ Pollut 2023, 320, 121065, doi: 10.1016/j.envpol.2023.121065.
9. Gelderblom W., Marasas W.: Controversies in Fumonisin Mycotoxicology and Risk Assessment. Hum Exp Toxicol 2012, 31, 215–235, doi: 10.1177/0960327110395338.
10. Gelineau-van Waes J.: Chapter 47, Fumonisins. In: *Reproductive and Developmental Toxicology*, Third Edition, edited by R.C. Gupta, Academic Press, Cambridge, MA, USA, 2022, pp. 955–981, doi: 10.1016/B978-0-323-89773-0.00047-3.
11. Gelineau-van Waes J., Voss K.A., Stevens V.L., Speer M.C., Riley R.T.: Chapter 5, Maternal Fumonisin Exposure as a Risk Factor for Neural Tube Defects. In: *Advances in Food and Nutrition Research*, Volume 56, edited by S.L. Taylor, Elsevier, New York, NY, USA, 2009, pp. 145–181, doi: 10.1016/S1043-4526(08)00605-0.
12. Hassan M.G., Horenberg A.L., Coler-Reilly A., Grayson W.L., Scheller E.L.: Role of the Peripheral Nervous System in Skeletal Development and Regeneration: Controversies and Clinical Implications. Curr Osteoporos Rep 2023, 21, 503–518, doi: 10.1007/s11914-023-00815-5.
13. Howard P.C., Warbritton A., Voss K.A., Lorentzen R.J., Thurman J.D., Kovach R.M., Bucci T.J.: Compensatory Regeneration as a Mechanism for Renal Tubule Carcinogenesis of Fumonisin B1 in the F344/N/Nctr BR Rat. Environ Health Perspect 2001, 109, 309–314, doi: 10.1289/ehp.01109s2309.
14. Kamle M., Mahato D.K., Devi S., Lee K.E., Kang S.G., Kumar P.: Fumonisins: Impact on Agriculture, Food, and Human Health and Their Management Strategies. Toxins 2019, 11, 328, doi: 10.3390/toxins11060328.
15. Kras K., Rudyk H., Muszyński S., Tomaszewska E., Dobrowolski P., Kushnir V., Muzyka V., Brezvyn O., Arciszewski M.B., Kotsyumbas I.: Morphology and Chemical Coding of Rat Duodenal Enteric Neurons following Prenatal Exposure to Fumonisins. Animals 2022, 12, 1055, doi: 10.3390/ani12091055.
16. Lebepe-Mazur S., Bal H., Hopmans E., Murphy P., Hendrich S.: Fumonisin B1 is fetotoxic in rats. Vet Hum Toxicol 1995, 37, 126–130.
17. Liu X., Liu H., Xiong Y., Yang L., Wang C., Zhang R., Zhu X.: Postmenopausal osteoporosis is associated with the regulation of SP, CGRP, VIP, and NPY. Biomed Pharmacother 2018, 104, 742–750, doi: 10.1016/j.biopha.2018.04.044.
18. Lumsangkul C., Chiang H.-I., Lo N.-W., Fan Y.-K., Ju J.-C.: Developmental Toxicity of Mycotoxin Fumonisin B1 in Animal Embryogenesis: An Overview. Toxins 2019, 11, 114, doi: 10.3390/toxins11020114.
19. Marasas W.F.O., Riley R.T., Hendricks K.A., Stevens V.L., Sadler T.W., Gelineau-van Waes J., Missmer S.A., Cabrera J., Torres O., Gelderblom W.C.A., Allegood J., Martínez C., Maddox J., Miller J.D., Starr L., Sullards M.C., Roman A.V., Voss K.A., Wang E., Merrill A.H.: Fumonisins Disrupt Sphingolipid Metabolism, Folate Transport, and Neural Tube Development in Embryo Culture and In Vivo: A Potential Risk Factor for Human Neural Tube Defects among Populations Consuming Fumonisin-Contaminated Maize. J Nutr 2004, 134, 711–716. doi: 10.1093/jn/134.4.711.

20. Marques S.I., Carmo H., Carvalho F., Sá S.I., Silva J.P.: A Semi-Automatic Method for the Quantification of Astrocyte Number and Branching in Bulk Immunohistochemistry Images. Int J Mol Sci 2023, 24, 4508, doi: 10.3390/ijms24054508.
21. Niedermair T., Schirner S., Seebröker R., Straub R.H., Grässel S.: Substance P modulates bone remodeling properties of murine osteoblasts and osteoclasts. Sci Rep 2018, 8, 9199, doi: 10.1038/s41598-018-27432-y.
22. O'Donnell K.J., Meaney M.J.: Fetal Origins of Mental Health: The Developmental Origins of Health and Disease Hypothesis. Am J Psychiatry 2017, 174, 319–328, doi: 10.1176/appi.ajp.2016.16020138.
23. Rao Z.-X., Tokach M.D., Woodworth J.C., DeRouchey J.M., Goodband R.D., Calderón H.I., Dritz S.S.: Effects of Fumonisin-Contaminated Corn on Growth Performance of 9 to 28 kg Nursery Pigs. Toxins 2020, 12, 604, doi: 10.3390/toxins12090604.
24. Riley R.T., Showker J.L., Owens D.L., Ross P.F.: Disruption of sphingolipid metabolism and induction of equine leukoencephalomalacia by *Fusarium proliferatum* culture material containing fumonisin B2 or B3. Env Toxicol Pharmacol 1997, 3, 221–228, doi: 10.1016/S1382-6689(97)00015-X.
25. Ross P.F., Ledet A.E., Owens D.L., Rice L.G., Nelson H.A., Osweiler G.D., Wilson T.M.: Experimental Equine Leukoencephalomalacia, Toxic Hepatosis, and Encephalopathy Caused by Corn Naturally Contaminated with Fumonisins. J Vet Diagn Invest 1993, 5, 69–74, doi: 10.1177/104063879300500115.
26. Rudyk H., Tomaszewska E., Kotsyumbas I., Muszyński S., Tomczyk-Warunek A., Szymańczyk S., Dobrowolski P., Wiącek D., Kamiński D., Brezvyn O.: Bone Homeostasis in Experimental Fumonisins Intoxication of Rats. Ann Anim Sci 2019, 19, 403–419, doi: 10.2478/aoas-2019-0003.
27. Rudyk H., Tomaszewska E., Arciszewski M.B., Muszyński S., Tomczyk-Warunek A., Dobrowolski P., Donaldson J., Brezvyn O., Kotsyumbas I.: Histomorphometrical Changes in Intestine Structure and Innervation Following Experimental Fumonisins Intoxication in Male Wistar Rats. Pol J Vet Sci 2020, 23, 77–88, doi: 10.24425/pjvs.2020.132751.
28. Schindelin J., Arganda-Carreras I., Frise E., Kaynig V., Longair M., Pietzsch T., Preibisch S., Rueden C., Saalfeld S., Schmid B., Tinevez J.-Y., White D.J., Hartenstein V., Eliceiri K., Tomancak P., Cardona A.: Fiji: an open-source platform for biological-image analysis. Nat Methods 2012, 9, 676–682, doi: 10.1038/nmeth.2019.
29. Shih C., Bernard G.W.: Neurogenic Substance P Stimulates Osteogenesis In Vitro. Peptides 1997, 18, 323–326, doi: 10.1016/S0196-9781(96)00280-X.
30. Spieker J., Ackermann A., Salfelder A., Vogel-Höpker A., Layer P.G.: Acetylcholinesterase Regulates Skeletal *In Ovo* Development of Chicken Limbs by ACh-Dependent and -Independent Mechanisms. PLoS One 2016, 11, e0161675, doi: 10.1371/journal.pone.0161675.
31. Steverink J.G., Oostinga D., Van Tol F.R., Van Rijen M.H.P., Mackaaij C., Verlinde-Schellekens S.A.M.W., Oosterman B.J., Van Wijck A.J.M., Roeling T.A.P., Verlaan J.-J.: Sensory Innervation of Human Bone: An Immunohistochemical Study to Further Understand Bone Pain. J Pain 2021, 22, 1385–1395, doi: 10.1016/j.jpain.2021.04.006.
32. Stockmann-Juvala H., Savolainen K.: A review of the toxic effects and mechanisms of action of fumonisin B1. Hum Exp Toxicol 2008, 27, 799–809, doi: 10.1177/0960327108099525.
33. Stoev S.D.: Foodborne Mycotoxicoses, Risk Assessment and Underestimated Hazard of Masked Mycotoxins and Joint Mycotoxin Effects or Interaction. Env Toxicol Pharmacol 2015, 39, 794–809, doi: 10.1016/j.etap.2015.01.022.
34. Tomaszewska E., Rudyk H., Dobrowolski P., Donaldson J., Świetlicka I., Puzio I., Kamiński D., Wiącek D., Kushnir V., Brezvyn O., Muzyka V., Doraczyńska R., Muszyński S., Kotsyumbas I.: Changes in the Intestinal Histomorphometry, the Expression of Intestinal Tight Junction Proteins, and the Bone Structure and Liver of Pre-Laying Hens Following Oral Administration of Fumonisins for 21 Days. Toxins 2021, 13, 375, doi: 10.3390/toxins13060375.
35. Tomaszewska E., Rudyk H., Muszyński S., Hułas-Stasiak M., Leszczyński N., Mielnik-Błaszczak M., Donaldson J., Dobrowolski P.: Prenatal Fumonisin Exposure Impairs Bone Development via Disturbances in the OC/Leptin and RANKL/RANK/OPG Systems in Weaned Rat Offspring. Int J Mol Sci 2023, 24, 8743, doi: 10.3390/ijms24108743.
36. Tomaszewska E., Rudyk H., Świetlicka I., Hułas-Stasiak M., Donaldson J., Arczewska M., Muszyński S., Dobrowolski P., Mielnik-Błaszczak M., Arciszewski M.B., Kushnir V., Brezvyn O., Muzyka V., Kotsyumbas I.: Trabecular Bone Parameters, TIMP-2, MMP-8, MMP-13, VEGF Expression and Immunolocalization in Bone and Cartilage in Newborn Offspring Prenatally Exposed to Fumonisins. Int J Mol Sci 2021, 22, 12528, doi: 10.3390/ijms222212528.
37. Tomaszewska E., Rudyk H., Świetlicka I., Hułas-Stasiak M., Donaldson J., Arczewska M., Muszyński S., Dobrowolski P., Puzio I., Kushnir V., Brezvyn O., Muzyka V., Kotsyumbas I.: The Influence of Prenatal Fumonisin Exposure on Bone Properties, as well as OPG and RANKL Expression and Immunolocalization, in Newborn Offspring Is Sex and Dose Dependent. Int J Mol Sci 2021, 22, 13234, doi: 10.3390/ijms222413234.
38. Tomaszewska E., Rudyk H., Wojtysiak D., Donaldson J., Muszyński S., Arciszewski M.B., Lisova N., Brezvyn O., Puzio I., Abramowicz B., Pawłowska-Olszewska M., Kotsyumbas I., Dobrowolski P.: Basal Blood Morphology, Serum Biochemistry, and the Liver and Muscle Structure of Weaned Wistar Rats Prenatally Exposed to Fumonisins. Animals 2022, 12, 2353, doi: 10.3390/ani12182353.
39. Tsunoda M., Dugyala R.R., Sharma R.P.: Fumonisin B1-induced increases in neurotransmitter metabolite levels in different brain regions of BALB/c mice. Comp Biochem Physiol C 1998, 120, 457–465, doi: 10.1016/S0742-8413(98)10061-0.
40. Wan Q., Qin W., Ma Y., Shen M., Li J., Zhang Z., Chen J., Tay F.R., Niu L., Jiao K.: Crosstalk between Bone and Nerves within Bone. Adv Sci 2021, 8, 2003390, doi: 10.1002/advs.202003390.
41. Yoo H.-S., Norred W.P., Showker J., Riley R.T.: Elevated Sphingoid Bases and Complex Sphingolipid Depletion as Contributing Factors in Fumonisin-Induced Cytotoxicity. Toxicol Appl Pharmacol 1996, 138, 211–218, doi: 10.1006/taap.1996.0119.